PCCP

Physical Chemistry Chemical Physics

This paper is published as part of a PCCP Themed Issue on:

Physical Chemistry of Biomolecular Motors and Machines
Guest Editor: Anatoly Kolomeisky (Rice University)

Papers

Enhancement of cargo processivity by cooperating molecular motors

Filippo Posta,[a] Maria R. D'Orsogna[b] and Tom Chou*[c]

Received 13th January 2009, Accepted 1st April 2009
First published as an Advance Article on the web 11th May 2009
DOI: 10.1039/b900760c

Cellular cargo can be bound to cytoskeletal filaments by one or more active or passive molecular motors. Recent experiments have shown that the presence of auxiliary, nondriving motors results in an enhanced processivity of the cargo, compared to the case of a single active driving motor alone. We model the observed cooperative transport process using a stochastic model that describes the dynamics of two molecular motors, an active one that moves cargo unidirectionally along a filament track, and a passive one that acts as a tether. Analytical expressions obtained from our analysis are fit to experimental data to estimate the microscopic kinetic parameters of our model. Our analysis reveals two qualitatively distinct processivity-enhancing mechanisms: the passive tether can decrease the typical detachment rate of the active motor from the filament track or it can increase the corresponding reattachment rate. Comparing analytical results with experimental data, we can show unambiguously that in the case of kinesin transport on microtubules, a higher average run length arises mainly from the ability of the passive motor to keep the cargo close to the filament, enhancing the reattachment rate of recently detached active kinesin motors. On the other hand, in the case of myosin-driven transport along actin, the passive motor tightly tethers the cargo to the filament, suppressing the detachment rate of the active myosin.

1. Introduction

To carry out its functions, a living cell requires the precise spatiotemporal organization of many macromolecules. Trafficking of molecules within the cytoplasm can be mediated by distinct processes including diffusion, polymerization, and active transport.[1] A variety of transport mechanisms may arise from the physical properties of the diverse cargoes being transported. For example, in the case of large cargoes such as organelles, mRNA or virus particles, diffusion may not be sufficiently fast nor be spatially controlled. These cargoes are often transported by motor proteins that processively move to and from the nucleus along specific cytoskeletal filaments.[2]

The cytoskeleton is typically composed of three types of filaments: microfilaments (*e.g.* actin), microtubules (*e.g.* tubulin α and β), and intermediate filaments (*e.g.* lamins).[3] Molecular motors most often associate with and process cargo along actin and microtubules.[4] These two filament types are structurally very different from each other. Microtubules (MT) are thicker (25 nm diameter) and have a specific radial orientation with respect to the cell nucleus. Actin filaments are more randomly distributed near the periphery of the cell, and are less thick (8 nm diameter) than MTs.[2,3] Moreover, filaments are directional. The ends of a microtubule are structurally different and labelled "positive" or "negative," while the ends of actin filaments are "pointed" or "barbed." Accordingly, there are different types of motor proteins associated with not only different filament types, but with the direction of transport along these filaments. The MT-specific motor proteins are kinesins (*e.g.*, kinesin I, II) that can move along MTs away from the nucleus on the positive direction, and dyneins that move in the opposite direction towards the negative end of a microtubule.[5] Various forms of the actin-specific motor myosin transport cargo toward the barbed (*e.g.* myoV) or pointed (*e.g.* myoVI) ends.[6,7] Since each motor is highly selective, and cargoes need to be moved on both directions of each filament, there are other proteins/cofactors that facilitate molecular transport by associating with specific motors and filaments. For example, dynactin is a cofactor of dynein that enhances both the processivity of dynein and its affinity to certain cargoes.[5]

Single molecule imaging methods have been pivotal in the experimental study of molecular motor dynamics.[8,9] Such advanced techniques have allowed researchers to dissect various aspects of molecular motor mediated transport.[10–15] The identification of motor proteins, their structure and properties have also led to several theoretical studies[16–19] that have further improved our understanding of how a single motor protein is able to move a cargo along a cytoskeletal filament.

Since many associated proteins/cofactors affect transport dynamics,[4] experimental and theoretical investigations of model systems that include only one motor and the tracks on which they bind do not yield a complete description of molecular motor based transport *in vivo*. Therefore, other recent studies have focused on how cooperativity among different molecular motors can facilitate cargo transport along straight, branched, and intersecting cytoskeletal

[a] *Dept. Biomathematics, UCLA, Los Angeles, CA. E-mail: fposta@ucla.edu*
[b] *Dept. Mathematics, CalState-Northridge, Los Angeles, CA. E-mail: dorsogna@csun.edu*
[c] *Dept. Biomathematics, UCLA, Los Angeles, CA. E-mail: tomchou@ucla.edu*

filaments.[7,20,21] In the experiments of Ali *et al.*[22,23] the cargoes were fluorescently labeled quantum dots (Qdots)[24] simultaneously attached to one kinesin and one myoV motor. While analyzing the dynamics of myoV transport in the presence of both actin and MT filaments, the authors discovered that myoV, besides processing along actin, is also able to associate with, and diffuse along microtubules. In further work,[23] the same authors showed that when both myoV and kinesin motors are attached to a single cargo, the processivity of the entire assembly is increased on both MT and actin filaments.

In this paper, we develop a stochastic model for the cooperative enhancement of kinesin and myoV as reported in ref. 23. Related stochastic models, both discrete and continuous have been effectively used to model the dynamics[18,25] and cooperativity[26] of single motors. These stochastic models describe the stepping dynamics of typically two-headed molecular motors (*e.g.* myoV or kinesin) that walk hand-over-hand along the filament, where the trailing and the leading heads exchange roles at each step. In our analysis, we take a coarser approach by treating the entire kinesin-myoV-cargo complex as a single structure that can exist in four possible states corresponding to different motor-filament association states. We extract and discuss probability density distributions for run length and times, as well as the corresponding means. In the Analysis & Discussion section, we fit the model to the experimental results from refs. 22 and 23. The fitting highlights a qualitative difference between cargo transport on actin and microtubules. We also discuss the dependence upon the initial conditions of the system and perform a sensitivity analysis on the unknown parameters.

2. Stochastic multistate transport model

Consider the molecular transport system of a cargo with two motor-proteins attached, one that acts as an active motor (*e.g.* kinesin on MT) and one that acts as a passive motor or tether (*e.g.* myoV on MT). We denote the state of the engine σ_a and of the passive tether σ_p by an ordered pair $\sigma = (\sigma_a,\sigma_p)$, where $\sigma_{a,p} = 1$ if the active/passive motor is attached to the filament track and where $\sigma_{a,p} = 0$ otherwise. Using this notation, state $\sigma = (1,1)$ corresponds to the case where both engine and tether attach cargo to the filament. State (1,0) represents a cargo complex whose engine is attached, but where the tether has detached from the filament (although it remains attached to the cargo). Conversely, (0,1) denotes the case where the engine has detached from the filament, but the tether still holds the cargo on the track. Finally, when both motors have detached from the filament, the complex reaches the (0,0) state. The states of the cargo system are schematically shown in Fig. 1. We only consider states in which, at any given time, at most only one active motor and one passive motor tether can attach a cargo to a filament. This assumption is reasonable because the procedure used in ref. 23 for motor attachment predicts that 95% of the Qdots used as cargo have only one active motor attached. While there are no predictions about the number of tethers attached to the cargo, the relatively small size of the Qdots used in the experiments ($\sim$15 nm diameter) suggests that simultaneous attachment of an active motor and multiple tethers is highly unlikely.

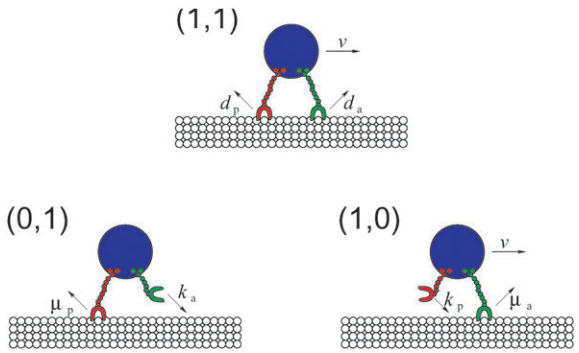

Fig. 1 Schematic of movement along a filament track of a cargo (blue circle) with both an active (green) and passive (red) motors attached. Each illustration represents one of three possible states the cargo complex can be in before detachment, together with the rate constants that lead the system out of a state. Note that the complex moves processively only if the active motor is attached. Only in state (0,1) can the system diffuse.

The cargo complex can move processively along a filament only if the active motor is attached to both the cargo and the filament. In our notation, this corresponds to states with a first index of one, *e.g.* (1,1) or (1,0). In state (0,1), the cargo is either diffusing or immobile, depending on the property of the passive motor. Within this context, we can write the Master equation for the probability density function $P_\sigma(x,t)$ that the motor–cargo complex is in a state σ between position x and $x + dx$ at time t:

$$\frac{\partial P_\sigma(x,t)}{\partial t} + v_\sigma \frac{\partial P_\sigma(x,t)}{\partial x} = D_\sigma \frac{\partial^2 P_\sigma(x,t)}{\partial x^2} + \sum_{\sigma'} [W(\sigma,\sigma')P_{\sigma'}(x,t) - W(\sigma',\sigma)P_\sigma(x,t)]. \quad (1)$$

Here, v_σ is the velocity of the cargo in state σ. This velocity will depend on the specific properties of the motor-protein and on any externally applied forces. For example, as has been well established under many experimental conditions,[14,21] opposing forces applied to motor-driven cargoes decrease their velocity linearly.

Consistent with observations, we set the diffusion constant $D_\sigma = 0$ in eqn (1) when an active, driving motor is attached, suppressing random diffusional motion. Conversely, when only a passive tether is attached, the motion of the cargo is Brownian and $D_\sigma \geq 0$.

The last term in eqn (1) represents transitions among binding states σ. The corresponding rates $W(\sigma,\sigma')$ are assumed to be constant and are defined in Table 1. Note that we make the physically reasonable assumption that a cargo complex in state (1,1) cannot have both motors detach simultaneously from the filament track, allowing no transition between state (1,1) and (0,0).

We will analyze the model given by eqn (1) by defining the probability density vector $\mathbf{P}(x,t) = (P_{(0,0)}, P_{(0,1)}, P_{(1,0)}, P_{(1,1)})^T$. If we assume that the filament track is infinitely long and that the cargo is at position $x = 0$ at initial time $t = 0$, the initial condition is $\mathbf{P}(x,t = 0) = (0,\alpha,\beta,1-\alpha-\beta)^T\delta(x)$, where α is the probability that the cargo complex is initially bound to the filament only by the passive tether and β is the probability that

Table 1 Description of transition rates $W(\sigma,\sigma')$ in eqn (1)

State transition	Rate	Description
(1,1) → (0,1)	d_a	Detachment rate of motor from motor–tether complex
(1,1) → (1,0)	d_p	Detachment rate of tether from motor–tether complex
(0,1) → (1,1)	k_a	Attachment rate of motor to tether-only complex
(1,0) → (1,1)	k_p	Attachment rate of tether to motor-only complex
(1,0) → (0,0)	μ_a	Detachment rate of motor from motor-only complex
(0,1) → (0,0)	μ_p	Detachment rate of tether from tether-only complex

the cargo complex is initially bound only to the active motor. While it is experimentally difficult to quantify α and β, it is relatively straightforward to determine how our main results for residence times and run lengths depend on the initial conditions. We can therefore establish, *a posteriori*, the importance of α,β in the measured results. Thus, by studying how certain estimated quantities depend on the initial conditions, we can determine the significance and usefulness of experimentally pinpointing the exact values of α and β.

The analysis is facilitated by defining the Laplace transform in time $\tilde{\mathbf{P}}(x,s) = \int_0^\infty \mathbf{P}(x,t)e^{-st}\,\mathrm{d}t$, and by taking the dual Laplace–Fourier transform of eqn (1):

$$s\hat{\mathbf{P}}(q,s) - \begin{pmatrix} 0 \\ \alpha \\ \beta \\ 1-\alpha-\beta \end{pmatrix} + \begin{pmatrix} 0 & 0 & 0 & 0 \\ 0 & D_p q^2 + iqv_p & 0 & 0 \\ 0 & 0 & D_a + iqv_a & 0 \\ 0 & 0 & 0 & D_{ap} + iqv_{ap} \end{pmatrix} \hat{\mathbf{P}} \quad (2)$$

$$= \begin{pmatrix} 0 & \mu_p & \mu_a & 0 \\ 0 & -k_a - \mu_p & 0 & d_a \\ 0 & 0 & -k_p - \mu_a & d_p \\ 0 & k_a & k_p & -d_a - d_p \end{pmatrix} \hat{\mathbf{P}},$$

imposing these physical constraints, we solve the Master equation to construct analytical expressions for the run lengths and run times. We will use these results to compare our model with experimental data from ref. 23.

2.1 Run length, run time and rest distributions

In this section we derive probability distribution functions (PDF) for the run length $P_{\mathrm{length}}(X)$, the run time $P_{\mathrm{time}}(T)$, the motor-driven run length $P_{\mathrm{active}}(X)$, and the duration of the rest state, where only the passive motor is attached to the filament, $P_{\mathrm{passive}}(T)$. To find the run length and time distributions, we define the cargo detachment flux density within positions x and $x + \mathrm{d}x$ at time t as follows:

$$J_{\mathrm{ap}}(x,t) = \mu_a P_{(1,0)}(x,t) + \mu_p P_{(0,1)}(x,t). \quad (3)$$

The probability distribution function $P_{\mathrm{length}}(X)$ for the run length X of a motor–tether complex detaching from the filament track between positions $x = X$ and $x = X + \mathrm{d}X$, for any time, can be found from the time integral of $J_{\mathrm{ap}}(x = X,t)$ as

$$P_{\mathrm{length}}(\mathrm{X}) = \int_0^\infty J_{\mathrm{ap}}(X,t)\mathrm{d}t = \tilde{J}_{\mathrm{ap}}(X, s = 0). \quad (4)$$

Here, following the notation introduced for $\mathbf{P}(x,t)$, $\tilde{J}_{\mathrm{ap}}(x,s)$ denotes the Laplace transform of $J_{\mathrm{ap}}(x,t)$ and $\hat{J}_{\mathrm{ap}}(q,s)$ its dual Laplace–Fourier transform. We also introduce the notation $\bar{J}_{\mathrm{ap}}(q,t)$ to denote the Fourier transform of $J_{\mathrm{ap}}(x,t)$ which will be used below to evaluate the run time distribution. Upon solving algebraically for $\hat{\mathbf{P}}(q,s)$ in eqn (2), we construct the corresponding $\hat{J}_{\mathrm{ap}}(q,s = 0)$

$$\hat{J}_{\mathrm{ap}}(q,s=0) = \frac{i(D_p d_p q^2 \mu_a + d_p \mu_a (k_a + \mu_p) + d_a \mu_p (k_p + \mu_a - iqv_a))}{d_a(D_p q^2 + \mu_p)(ik_p + i\mu_a + qv_a) + (D_p q^2 + k_a + \mu_p)[qv_a(k_p + \mu_a - iqv_a) + d_p(i\mu_a + qv_a)]}, \quad (5)$$

where $\hat{\mathbf{P}}(q,s) = \int_0^\infty \tilde{\mathbf{P}}(x,s)e^{-iqx}\,\mathrm{d}x$. In the above equation, and in the remainder of the paper, we use the subscripts a, p and ap to indicate the quantities and/or expressions that are characteristic of a transport complex consisting of an active motor only (a), a passive motor only (p) or both (ap). In eqn (2), we assumed that motion is purely convective when an active motor attaches the cargo to the filament, and therefore, we set $D_a = D_{ap} = 0$. As indicated by the experimental data in ref. 23, the passive tether does not noticeably affect the transport velocity of an active motor. Therefore, we also set $v_{ap} = v_a$, where v_{ap} is the intrinsic velocity of cargo in the state (1,1). Finally, since the passive motor acting as a simple tether cannot induce drift along a filament track, we set $v_p = 0$. After which can be decomposed as a sum of partial fractions

$$\hat{J}_{\mathrm{ap}}(q,s=0) = \sum_{j=1}^{4} \frac{iA_j}{(q - iq_j)}. \quad (6)$$

Here, iq_j are the imaginary roots of the denominator in eqn (5) and iA_j the coefficients of the corresponding partial fraction. Both q_j and A_j are functions of the transition rates and diffusion constants. Finally, upon taking the inverse Fourier transform of eqn (6) we find

$$P_{\mathrm{length}}(X) = \sum_{j=1}^{4} A_j \exp[-|q_j|X]\Theta(Xq_j/|q_j|), \quad (7)$$

where $\Theta(y)$ is the Heaviside function. The PDF $P_{\text{length}}(X)$ is evaluated numerically and plotted as a function of X in Fig. 2(a) for the specific parameters listed in the Figure caption. Some of these parameters are taken from Ali *et al.*,[23] while others are fixed by fitting to experimental data, as described in the following sections.

Similarly, we compute the PDF $P_{\text{time}}(T)$ for the run time of the motor–tether complex detaching from the filament between time $t = T$ and $t = T + \mathrm{d}T$

$$P_{\text{time}}(\mathrm{T}) = \int_{-\infty}^{\infty} J_{\text{ap}}(x,T)\mathrm{d}x = \bar{J}_{\text{ap}}(q = 0, T). \qquad (8)$$

From eqn (2) we find

$$\hat{J}_{\text{ap}}(q=0,s) = \frac{d_{\text{a}}\mu_{\text{p}}(k_{\text{p}}+\mu_{\text{a}}+s) + d_{\text{p}}\mu_{\text{a}}(k_{\text{a}}+\mu_{\text{p}}+s)}{d_{\text{p}}(\mu_{\text{a}}+s)(k_{\text{a}}+\mu_{\text{p}}+s) + (k_{\text{p}}+\mu_{\text{a}}+s)[d_{\text{a}}(\mu_{\text{p}}+s) + s(k_{\text{a}}+\mu_{\text{p}}+s)]}. \qquad (9)$$

The denominator in eqn (9) is a cubic in s and admits only negative roots. If we denote them by $s = -s_j$ with $s_j > 0$, the dual Laplace–Fourier transform of the detachment flux can be expressed as

$$\hat{J}(q=0,s) = \sum_{j=1}^{3} \frac{B_j}{s+s_j}. \qquad (10)$$

Here, both s_j and the coefficients B_j are functions of the transition rates. Upon taking the inverse Laplace transform of eqn (10), we find

$$P_{\text{time}}(T) = \sum_{j=1}^{3} B_j e^{-s_j T}. \qquad (11)$$

In Fig. 2(b), we plot $P_{\text{time}}(T)$ for the same parameters used in Fig. 2(a).

We now evaluate the PDF $P_{\text{active}}(X)$ for the run length of a processive motor. Following the previous analysis, the probability density flux $J_{\text{a}}(x,t)$ out of the state where the driving motor is attached can be expressed as

$$J_{\text{a}}(x,t) = \mu_{\text{a}}P_{(1,0)}(x,t) + d_{\text{a}}P_{(1,1)}(x,t). \qquad (12)$$

Since the final two states $(0,\sigma_{\text{p}})$ are both absorbing, we must also set $k_{\text{a}} = 0$ in the evaluation of $J_{\text{a}}(x,t)$ and use the initial condition $\alpha = 0$. The Fourier–Laplace transform of $J_{\text{a}}(x,t)$ is given by

$$\hat{J}_{\text{a}}(q,s) = \frac{d_{\text{p}}\mu_{\text{a}} + d_{\text{a}}(k_{\text{p}}+\mu_{\text{a}}-iqv_{\text{a}})}{d_{\text{a}}(k_{\text{p}}+\mu_{\text{a}}-iqv_{\text{a}}) - i[qv_{\text{a}}(k_{\text{p}}+\mu_{\text{a}}-iqv_{\text{a}}) + d_{\text{p}}(i\mu_{\text{a}}+qv_{\text{a}})]}, \qquad (13)$$

which results in the active motor run length distribution

$$P_{\text{active}}(X) = \sum_{j=1}^{2} C_j e^{-q'_j X} H(X), \qquad (14)$$

where iq_{j}' ($q_j' > 0$) are the roots of the denominator in eqn (13). Finally, the probability distribution function $P_{\text{passive}}(T)$ for a cargo complex to be tethered only by the passive motor in state (0,1) can be found from the passive state detachment flux density

$$J_{\text{p}}(x,t) = (\mu_{\text{p}} + k_{\text{a}})P_{(0,1)}(x,t), \qquad (15)$$

by setting the entry rate into this state $d_{\text{a}} = 0$, and by assuming $\beta = 0$ as initial condition. As done for the previous cases, we find that $P_{\text{passive}}(T)$ is a simple decaying exponential

$$P_{\text{passive}}(T) = (k_{\text{a}} + \mu_{\text{p}})e^{-(k_{\text{a}}+\mu_{\text{p}})T}. \qquad (16)$$

In the case of cargoes transported along actin, myoV is tightly bound and $D_{\text{p}} = 0$. $P_{\text{passive}}(T)$ is then the time distribution for resting cargoes.

2.2 Mean run lengths and run times

Experiments by Ali *et al.*[23] show significant increases in the processivity of a cargo when it is also attached to a *passive* motor. Within our model, the measured processivity is equivalent to the mean run length, $\langle X_{\text{ap}}\rangle$. The latter, and in fact, all run length moments, can be found from our run length PDF

$$\begin{aligned}\langle X_{\text{ap}}^m\rangle &= \int_{-\infty}^{\infty} x^m P_{\text{length}}(x)\mathrm{d}x \\ &= \int_{-\infty}^{\infty}\left[\int_0^{\infty} J_{\text{ap}}(x,t)\mathrm{d}t\right]x^m\mathrm{d}x \\ &= \int_{-\infty}^{\infty} x^m[\mu_{\text{a}}\tilde{P}_{(1,0)}(x,s=0) + \mu_{\text{p}}\tilde{P}_{(0,1)}(x,s=0)]\mathrm{d}x \\ &= \left(i\frac{\partial}{\partial q}\right)^m \hat{J}_{\text{ap}}(q,s=0)|_{q=0}.\end{aligned} \qquad (17)$$

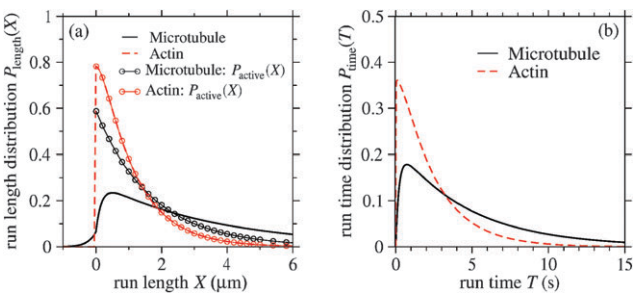

Fig. 2 (a) Run length probability distribution function (PDF) $P_{\text{length}}(X)$ for transport along microtubules and actin. Initial conditions are chosen with cargo initially in the $P_{(1,1)}$ state at $x = 0$ so that $\alpha = \beta = 0$. Parameters are chosen as $\mu_{\text{a}} = d_{\text{a}} = 0.52$, $\mu_{\text{p}} = 0.5$, $D_{\text{p}} = 0.1$, $k_{\text{a}} = 1.48$, $k_{\text{p}} = 1.0$, $dp = 0.58$, $v_{\text{a}} = 0.88$ in the case of microtubule transport, and $\mu_{\text{a}} = 0.61$, $d_{\text{a}} = 0.37$, $\mu_{\text{p}} = 100$, $D_{\text{p}} = k_{\text{a}} = 0$, $k_{\text{p}} = 1.0$, $d_{\text{p}} = 0.5$, $v_{\text{a}} = 0.46$ for motion along actin filaments. Note that due to non-zero diffusion in the case of transport along microtubules, the cargo can take on negative values of x. Since $D_{\text{p}} = 0$ for transport along actin filaments, cargo can only proceed along the $x > 0$ semi-axis. We also plot the PDF of the run lengths for cargoes in the active, processing state. For transport on actin filaments, the full run length PDF and the run length in the actively transported states are indistinguishable, while for transport along microtubules, significant time is spent in the nonprocessive, diffusive state such that P_{length} and P_{active} are qualitatively different. (b) Probability distribution function $P_{\text{time}}(T)$ for the case of cargo detachment along microtubules and actin. All parameters and initial conditions are chosen as in panel (a).

The moments of the cargo run times are similarly found:

$$\begin{aligned}\langle T_{\mathrm{ap}}^{m}\rangle &= \int_0^\infty t^m P_{\mathrm{time}}(t)\mathrm{d}t \\ &= \int_0^\infty \left[\int_{-\infty}^{\infty} J_{\mathrm{ap}}(x,t)\mathrm{d}x\right] t^m \mathrm{d}t \\ &= \int_0^\infty t^m[\mu_{\mathrm{a}}\,\bar{P}_{(1,0)}(q=0,t)+\mu_{\mathrm{p}}\,\bar{P}_{(0,1)}(q=0,t)]\mathrm{d}t \\ &= \left(-\frac{\partial}{\partial s}\right)^m \hat{J}_{\mathrm{ap}}(q=0,s)|_{s=0}.\end{aligned} \tag{18}$$

In the experiments of Ali *et al.*,[23] only the mean run lengths and mean run times are accurately measured. Therefore, we will focus on fitting our model to mean quantities. Using eqn (5) for $\hat{J}_{\mathrm{ap}}$, we explicitly find the *mean* run length

$$\langle X_{\mathrm{ap}}\rangle = v_{\mathrm{a}}\frac{(d_{\mathrm{p}}+k_{\mathrm{p}}+\mu_{\mathrm{a}}-\beta\mu_{\mathrm{a}})(k_{\mathrm{a}}+\mu_{\mathrm{p}})+d_{\mathrm{a}}\beta\mu_{\mathrm{p}}-\alpha[\mu_{\mathrm{p}}(k_{\mathrm{p}}+\mu_{\mathrm{a}})+d_{\mathrm{p}}\mu_{\mathrm{p}}]}{d_{\mathrm{a}}\mu_{\mathrm{p}}(k_{\mathrm{p}}+\mu_{\mathrm{a}})+d_{\mathrm{p}}\mu_{\mathrm{a}}(k_{\mathrm{a}}+\mu_{\mathrm{p}})}. \tag{19}$$

As expected, $\langle X_{\mathrm{ap}}\rangle$ is independent of any diffusion of the passive tether since diffusion on average does not contribute to the mean displacement. The mean run length is a monotonically decreasing function of α for all the physically realistic (*i.e.* positive) values of the model parameters. On the other hand, the dependence of $\langle X_{\mathrm{ap}}\rangle$ on β will be monotonically increasing (decreasing) if the term $d_{\mathrm{a}}\mu_{\mathrm{p}} - \mu_{\mathrm{a}}(k_{\mathrm{a}} + \mu_{\mathrm{p}})$ is positive (negative). The processivity of a cargo complex initially in state (1,0) (when $\beta = 1$) is greater than that of a cargo beginning in state (1,1) (when $\beta = 0$) only when the detachment rate d_{a} of the active motor from the state when both motors are attached is greater than $\mu_{\mathrm{a}}(1 + k_{\mathrm{a}}/\mu_{\mathrm{p}})$, where μ_{a} is the detachment rate of the active motor by itself.

Eqn (19) can be simplified by assuming that both motors are initially attached to the filament, the same initial condition used in the experiments of ref. 23. Setting ($\alpha = \beta = 0$) we find

$$\langle X_{\mathrm{ap}}\rangle = \frac{(k_{\mathrm{p}}+d_{\mathrm{p}}+\mu_{\mathrm{a}})(k_{\mathrm{a}}+\mu_{\mathrm{p}})v_{\mathrm{a}}}{\mu_{\mathrm{p}}d_{\mathrm{a}}(k_{\mathrm{p}}+\mu_{\mathrm{a}})+\mu_{\mathrm{a}}d_{\mathrm{p}}(k_{\mathrm{a}}+\mu_{\mathrm{p}})}. \tag{20}$$

As expected, $\langle X_{\mathrm{ap}}\rangle$ is a monotonically increasing function of k_{a}, k_{p} and v_{a}, and a monotonically decreasing function of d_{a}, d_{p}, μ_{a} and μ_{p}.

The expression for the moments of the density flux J_{a} out of the states where the motor is attached is analogous to eqn (17) with $P_{\mathrm{active}}(X)$ substituted for $P_{\mathrm{length}}(X)$. The mean run length of a cargo complex conditioned on being bound by an active motor is explicitly

$$\langle X_{\mathrm{a}}\rangle = v_{\mathrm{a}}\frac{\beta(d_{\mathrm{a}}-\mu_{\mathrm{a}})+(d_{\mathrm{p}}+k_{\mathrm{p}}+\mu_{\mathrm{a}})}{d_{\mathrm{p}}\mu_{\mathrm{a}}+d_{\mathrm{a}}(k_{\mathrm{p}}+\mu_{\mathrm{a}})}, \tag{21}$$

and is a monotonically increasing (decreasing) function of β if $d_{\mathrm{a}} > \mu_{\mathrm{a}}$ ($d_{\mathrm{a}} < \mu_{\mathrm{a}}$). As we will verify below, the corresponding mean time is simply $\langle T_{\mathrm{a}}\rangle = \langle X_{\mathrm{a}}\rangle/v_{\mathrm{a}}$. A simple analysis of eqn (21) reveals that if $\beta = 0$ the mean run length $\langle X_{\mathrm{a}}\rangle$ in states (1,σ_{p}) is a monotonically decreasing function of k_{p} and a monotonically increasing function of d_{p} if $d_{\mathrm{a}} > \mu_{\mathrm{a}}$. If $d_{\mathrm{a}} < \mu_{\mathrm{a}}$, the mean run length $\langle X_{\mathrm{a}}\rangle$ in state (1,σ_{p}) is a monotonically increasing function of k_{p} and a monotonically decreasing function of d_{p}. When the detachment rate of the active motor is independent of its state (*e.g.*, $\mu_{\mathrm{a}} = d_{\mathrm{a}}$), $\langle X_{\mathrm{a}}\rangle = v_{\mathrm{a}}/\mu_{\mathrm{a}}$ is independent of the initial conditions and the properties of the tether.

Finally, the mean run length of a cargo bound only by a passive tether (state (0,1)) can be computed from the first moment of eqn (16), yielding $\langle X_{\mathrm{p}}\rangle = 0$. This trivial result stems from the drift-free nature ($v_{\mathrm{p}} = 0$) of the (0,1) state. Using eqn (18) with $m = 1$, we can also find the mean run time for general initial conditions as

$$\langle T_{\mathrm{ap}}\rangle = \frac{(d_{\mathrm{a}}+k_{\mathrm{a}}+\mu_{\mathrm{p}}-\alpha\mu_{\mathrm{p}})(k_{\mathrm{p}}+\mu_{\mathrm{a}})+(d_{\mathrm{p}}-\beta\mu_{\mathrm{a}})(k_{\mathrm{a}}+\mu_{\mathrm{p}})+(\alpha d_{\mathrm{p}}-\beta d_{\mathrm{a}})(\mu_{\mathrm{a}}-\mu_{\mathrm{p}})}{d_{\mathrm{a}}(k_{\mathrm{p}}+\mu_{\mathrm{a}})\mu_{\mathrm{p}}+d_{\mathrm{p}}\mu_{\mathrm{a}}(k_{\mathrm{a}}+\mu_{\mathrm{p}})}. \tag{22}$$

The above estimate and all other moments in eqn (18) do not depend on the diffusion constant, since the latter influences detachment position and not its temporal occurrence. As in section 2, we can study the dependence of $\langle T_{\mathrm{ap}}\rangle$ on the kinetic parameters by considering the $\alpha = \beta = 0$ limit corresponding to the experimental setup of ref. 23:

$$\langle T_{\mathrm{ap}}\rangle = \frac{d_{\mathrm{p}}(k_{\mathrm{a}}+\mu_{\mathrm{p}})+(k_{\mathrm{p}}+\mu_{\mathrm{a}})(d_{\mathrm{a}}+k_{\mathrm{a}}+\mu_{\mathrm{p}})}{d_{\mathrm{a}}(k_{\mathrm{p}}+\mu_{\mathrm{a}})\mu_{\mathrm{p}}+d_{\mathrm{p}}\mu_{\mathrm{a}}(k_{\mathrm{a}}+\mu_{\mathrm{p}})}. \tag{23}$$

This expression is monotonically decreasing with respect to μ_{a} and μ_{p}, and can be used in conjunction with eqn (20) to obtain an expression for the mean velocity of cargo transport in presence of an active and a passive motor

$$\begin{aligned}\langle V_{\mathrm{ap}}\rangle &\equiv \frac{\langle X_{\mathrm{ap}}\rangle}{\langle T_{\mathrm{ap}}\rangle} \\ &= \frac{(k_{\mathrm{p}}+d_{\mathrm{p}}+\mu_{\mathrm{a}})(k_{\mathrm{a}}+\mu_{\mathrm{p}})v_{\mathrm{a}}}{d_{\mathrm{p}}(k_{\mathrm{a}}+\mu_{\mathrm{p}})+(k_{\mathrm{p}}+\mu_{\mathrm{a}})(d_{\mathrm{a}}+k_{\mathrm{a}}+\mu_{\mathrm{p}})} \le v_{\mathrm{a}}.\end{aligned} \tag{24}$$

This result indicates that even though states (1,1) and (1,0) drift with velocity v_{a}, the entire run consists of alternating phases of drifting and diffusive states, resulting in an average effective velocity $V_{\mathrm{ap}} \le v_{\mathrm{a}}$. The two velocities are similar only when active motor dissociation from state (1,1) is slow (*e.g.* $d_{\mathrm{a}} \ll 1$), and/or tether dissociation from state (0,1) is fast (*e.g.* $\mu_{\mathrm{p}} \gg 1$). From the above expression, one can estimate the ratio χ of convection times to diffusion times

$$\begin{aligned}\chi &= \frac{|V_{\mathrm{ap}}-v_{\mathrm{a}}|}{v_{\mathrm{a}}} \\ &= \frac{d_{\mathrm{a}}(k_{\mathrm{p}}+\mu_{\mathrm{a}})}{d_{\mathrm{p}}(k_{\mathrm{a}}+\mu_{\mathrm{p}})+(k_{\mathrm{p}}+\mu_{\mathrm{a}})(d_{\mathrm{a}}+k_{\mathrm{a}}+\mu_{\mathrm{p}})} \le 1.\end{aligned} \tag{25}$$

In order to evaluate the detachment time of the driving motor from the filament track, we consider the mean first passage time $\langle T_{\mathrm{a}}\rangle$ out of states (1,σ_{p}). In this case we impose $k_{\mathrm{a}} = 0$, $\alpha = 0$ and $m = 1$ in eqn (18) to verify that

$$\langle T_{\mathrm{a}}\rangle = \frac{\beta(d_{\mathrm{a}}-\mu_{\mathrm{a}})+(d_{\mathrm{p}}+k_{\mathrm{p}}+\mu_{\mathrm{a}})}{d_{\mathrm{p}}\mu_{\mathrm{a}}+d_{\mathrm{a}}(k_{\mathrm{p}}+\mu_{\mathrm{a}})} = \frac{\langle X_{\mathrm{a}}\rangle}{v_{\mathrm{a}}}. \tag{26}$$

This result stems from the fact that we are only considering processive runs, where the cargo complex travels at velocity v_a. If instead we consider a trajectory composed of both processive and diffusive runs, the effective speed will typically be smaller, as shown in eqn (25).

The above algebraic expressions for the mean length (*e.g.* eqn (19)) and duration (*e.g.* eqn (22)) of a run in various states constitute the main mathematical results of this section.

3. Analysis & discussion

Having obtained analytical expressions for the mean run length and duration, we can use experimental data from ref. 23 to estimate parameters within our model. Since only mean run length and run times can be obtained from the published data,[23] we first fit to these means to constrain our model parameters. Further refinement of parameters requires fitting to finer features of the PDFs, and will be discussed in the Summary and Conclusions. Since the experiments were performed on motors that process along microtubules and actin, we will divide the analysis into the two corresponding cases.

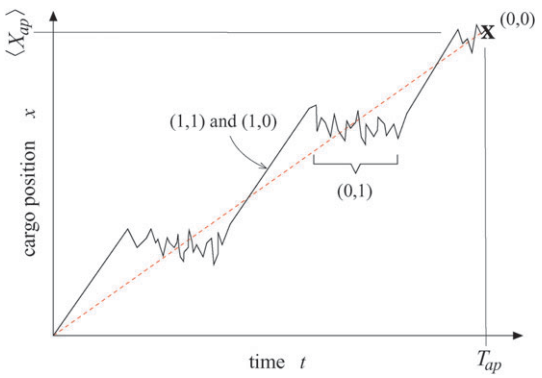

Fig. 3 A representative trajectory. The processive runs during states (1,1), (0,1) are assumed to have the same velocity independently of the state they are in. The depicted cargo movement is characterized by three processive runs, all with the same slope (*e.g.* same velocity) and three diffusive events due to the cargo complex being in state (0,1) before complete detachment at **X**. The dashed red line represents a straight trajectory that defines an effective velocity of a complete run before detachment.

3.1 Parameter fitting

In the absence of external forces v_a is constant, $v_p = 0$, and for fixed initial conditions, the model is characterized by 8 parameters. Only for a few of them it is possible to extract estimates from the available literature (see Table 2). However, we can use certain biophysical constraints stemming from ref. 23 to reduce the parameter space as much as possible. Throughout this subsection the analysis is performed with $\alpha = \beta = 0$.

3.1.1 myoV–kinesin transport on MT. Experimental results from ref. 23 show that the presence of a passive myoV motor, in addition to an active kinesin motor increases the typical run length of the cargo by two-fold and slightly decreases the velocity by $\sim$15%. The same data show that the velocity and mean run length of cargo in state (1,0) and state (1,1) are essentially the same. Fig. 3 is a graphical representation of a possible cargo trajectory showing three processive and three diffusive runs. Since all processive runs are observed to occur with the same velocity, the presence of the passive myosin does not affect the drive of the active kinesin motor. Therefore, both states (1,0) and (1,1) are indistinguishable within each processive run. These observations suggest that we can assume $d_a = \mu_a$ in eqn (1). We used this assumption and the values of v_a, μ_a from Table 2 to solve the system consisting of eqn (20) and eqn (23) with the constraints $\langle X_{ap} \rangle = 3.7$ μm and $T_{ap} = 5.0$ s obtained from the experimental results in ref. 23 for microtubular transport.

The solution of this system leads to a specific value of $k_a = 1.48\ s^{-1}$, implying an average diffusion time of $1/k_a = 0.68$ s, consistent with the experimental results in ref. 23. In fact, the average run length of a kinesin–myoV cargo complex on microtubules lasts about 5 s and covers twice the distance of a Qdot with only a single kinesin motor attached to it. Therefore, the typical cargo movement due to a kinesin/myoV motor consists of two processive steps (needing $\sim 2T_a = 4.4$ s, see ref. 23) and one or two diffusive

Table 2 Typical values of parameters and mathematical quantities for kinesin/myoV cargo transport

	Mean value	Physical definition	Ref.
$\langle X_a \rangle$	0.76 μm 1.7 μm	Mean run length of myoV on actin Mean run length of kinesin on MT	23
$\langle X_{ap} \rangle$	1.09 μm 3.7 μm	Mean run length of myoV-kinesin on actin Mean run length of myoV-kinesin on MT	23
v_a	0.46 μm s^{-1} 0.88 μm s^{-1}	Velocity of myoV on actin Velocity of kinesin on MT	23
μ_a	0.60 s^{-1} 0.51 s^{-1}	Detachment rate of myoV from actin Detachment rate of kinesin from MT	23
k_a	$>0.2\ s^{-1}$	Attachment rate of kinesin from MT	23
μ_p	$>0.02\ s^{-1}$	Detachment rate of myoV from MT	22, 23
D_p	0.11–0.26 $\mu m^2\ s^{-1}$	Diffusion of myoV on MT	22, 23

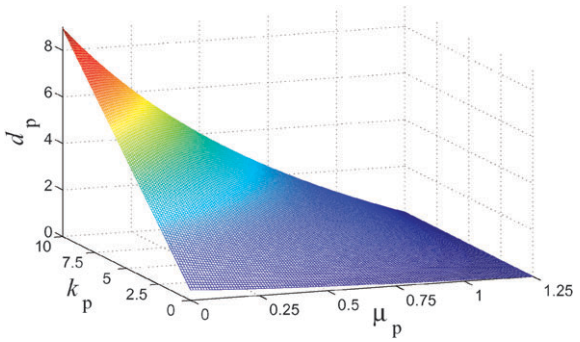

Fig. 4 Surface plot of the parameter space that satisfies the conditions of section 3.1.1 for the mean run length and first passage time. While both k_p and d_p can have values along the positive real line, μ_p has an upperbound. If $\mu_p > 1.25\ s^{-1}$ there are no physically realistic values of k_p and d_p that satisfy the conditions $\langle X_{ap}\rangle = 3.7$ and $T_{ap} = 5.0$. For this plot, $v_a = 0.88\ \mu m$, $\mu_a = d_a = 0.52\ s^{-1}$, $k_a = 1.48\ s^{-1}$.

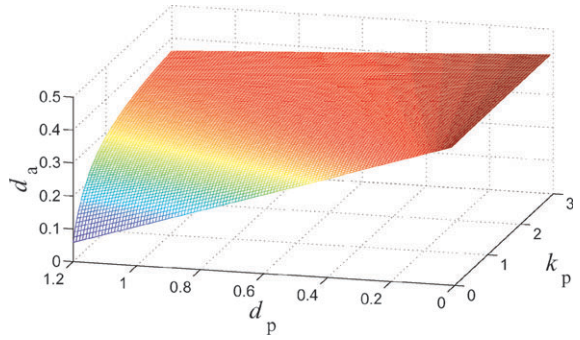

Fig. 5 Surface plot of the values of k_p, d_p, and d_a that satisfy the mean run-length expression in eqn (27) when, $v_a = 0.46\ \mu m$ and $\mu_a = 0.60\ s^{-1}$. For $k_p \ll d_p$, d_a tends to the value $0.42\ s^{-1}$. This value is equivalent to having a cargo complex consisting of only one active and no passive motor.

ones before detachment since we assumed that the cargo is initially in state (1,1). Given such observations, our obtained value of k_a is consistent with the experimental data. More specifically, it suggests that on average there will be only one single diffusive event in between two processive runs.

For the three remaining parameters we find that as long as $\mu_p < 1.25\ s^{-1}$, we can always find k_p and d_p that satisfy the physical constraints $\langle X_{ap}\rangle = 3.7\ \mu m$ and $T_{ap} = 5.0$ s. These results are shown in Fig. 4. The upper limit for μ_p implies an average diffusion time of about 0.8 s while in state (0,1) and before detachment. However, the experimental results in ref. 22 and 23 show an average diffusion time between 40 and 60 s in the absence of kinesin. The observed diffusion times are consistent with the value for k_a obtained above and suggest that the detachment of the cargo from the microtubule is most likely to happen while the motor is in state (1,0).

Overall, these results suggest that myoV increases the processivity of the cargo complex by keeping kinesin close enough to the track so that its reattachment is accelerated. The tethering by myoV occurs without reduction in the intrinsic velocity of kinesin.

3.1.2 myoV–kinesin transport on actin. The most striking finding observed using this experimental system is that the processivity is increased by the presence of a passive kinesin tether, but the average velocity remains unchanged, suggesting that the passive tether helps keep the active myoV attached to the filament track without affecting its velocity. In these experiments, one observes longer, uninterrupted processive transport, with rare punctuated moments of diffusive cargo motion. This suggests that the system is predominantly in states $(1,\sigma_p)$ and that once the active motor detaches, the whole cargo system does too. These observations are consistent with the structural/molecular attributes of this system, since the electrostatic forces between actin and kinesin are too weak to significantly reduce the myosin driven cargo velocity. Moreover, since actin filaments are thin, once myosin detaches, the detachment of kinesin is also fast. But if myosin holds kinesin proximal to the actin filament, the kinesin attachment rate is also fast, since free diffusion is hindered by the tether. Within this context $d_a \neq \mu_a$. We can also assume that $k_a = 0$ and that $\mu_p \to \infty$, leading to the following expressions for the mean run length and first passage time

$$\langle X_{ap}\rangle = \frac{(k_p + d_p + \mu_a)v_a}{d_a(k_p + \mu_a) + d_p\mu_a},$$
$$\langle T_{ap}\rangle = \frac{d_p + k_p + \mu_a}{d_a(k_p + \mu_a) + d_p\mu_a}. \quad (27)$$

The above expressions are the same as eqn (21) and eqn (26) for the particular choice of initial conditions that we have used throughout this section. Moreover, in these configurations the velocity is v_a. Therefore, the model is able to predict the observed experimental behavior. We can now use $\langle X_{ap}\rangle = 1.09\ \mu m$ and $T_{ap} = 2.59$ s (obtained from Table 1 in ref. 23) to plot the parameter space that satisfies either one of the expressions in eqn (27) but not both since they are redundant under the assumption $\langle V_{ap}\rangle = v_a$. Using the expression for the mean run length in eqn (27), we obtain the plot shown in Fig. 5. Here, we see that for $k_p \gg d_p$, d_a reaches a maximum value of $d_a = 0.42\ s^{-1}$. This quantity is smaller than μ_a, a result that confirms our interpretation that the increase in processivity is due to the tethers ability to prevent detachment of the active motor.

From the properties of actin transport discussed thus far, it seems natural to consider an "effective" detachment rate μ_{eff} that captures the dynamics of cargo transport in this case:

$$\mu_{eff} = f(\mu_a, \mu_p, k_p, d_a, d_p, v_a) = \frac{v_a}{\langle X_{ap}\rangle}. \quad (28)$$

From the results in ref. 23, we obtain $\mu_{eff} \approx 0.42\ s^{-1}$. This value is the same as the maximum value obtained above, implying that the overall effect of kinesin is to prevent myoV from detaching from the actin filament, without affecting the intrinsic myoV transport velocity.

3.2 Dependence on initial conditions

We now investigate how the model fits data as α and β in eqn (2) vary between zero and one. Based on the experimental methodology of ref. 23 we expect both α and β to be small. In

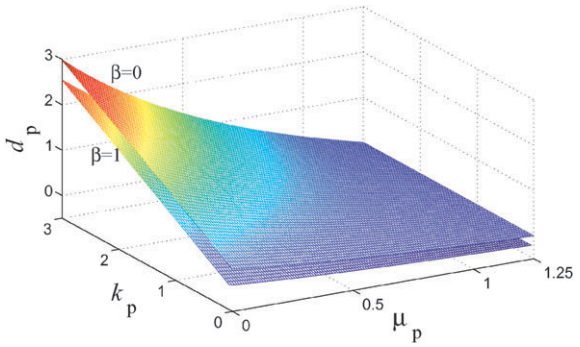

Fig. 6 Plot of the dependence of k_p, d_p and μ_p on β for transport along microtubules. The values of the other parameters are the same as the ones in Fig. 4. Increasing the number of cargo complexes in state (1,0) at time $t = 0$ leads to smaller values of tether detachment from state (1,1) for all values of k_p and μ_p.

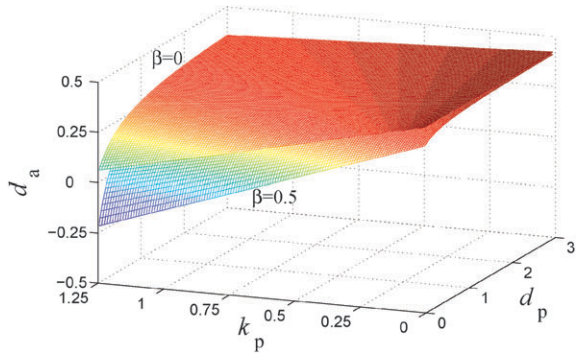

Fig. 7 Plot of the dependence of k_p, d_p, and d_a on β for transport along actin. The values of the other parameters are the same as the ones in Fig. 5. Increasing the number of cargo complexes in state (1,0) at time $t = 0$ leads to smaller values of active motor detachment rate from state (1,1). Moreover, some of the values of k_p and d_p lead to negative values of d_a although the limiting behavior for $k_p \ll d_p$ is still the same as for the case $\beta = 0$.

fact, only Qdots that show a displacement greater than 0.3 μm where included in the data, with shorter trajectories discarded, essentially reducing α to zero. The argument for β being small also relies upon the experimental methods of Ali *et al.*[23] To ensure that each Qdot had at most one active motor and at least a passive one attached to it, they prepared a solution where passive motors were in excess, with molar ratio 16 : 1.[23]

3.2.1 myoV–kinesin transport on MT. As discussed above, in the case of microtubular transport, we can use the approximation $d_a = \mu_a$. Unlike the case with simple initial conditions ($\alpha = \beta = 0$), including this constraint in eqn (19) and (22) does not yield a simple analytical solution for the mean run length and first passage time before detachment. Therefore, we performed a numerical study of the dependence on the initial conditions and found that for every choice of α and β there is only one value of k_a that satisfies the experimental results $\langle X_{ap} \rangle = 3.7$ μm and $T_{ap} = 5$ s. In addition, this value depends only on the initial fraction of cargoes in state (0,1) and not on β. In particular, k_a is a linear function of α, with slope $m = 1.26\ s^{-1}$, giving us a range of predicted values from $k_a = 1.48\ s^{-1}$ (if $\alpha = 0$) to $k_a = 2.74\ s^{-1}$ (if $\alpha = 1$). The increase of predicted k_a with α is not surprising since the higher the probability the systems starts in state (0,1), the faster the kinesin motor will have to bind to the microtubule to satisfy the given time constraint. Conversely, the values of the other free parameters in the model (*i.e.* d_p, μ_p, and k_p) depend only on the value of β. This dependence is shown in Fig. 6 for the limit cases $\beta = 0$ and $\beta = 1$ (in both cases $\alpha = 0$). From this plot we notice how an increase in the percentage of cargo complexes in state (0,1) at $t = 0$, shifts the parameter surface down along the d_p axis. As a result the parameter space itself in Fig. 6 is reduced, since any combination of parameters resulting in $d_p < 0$ is unphysical. From this analysis it seems that all possible initial conditions can explain the experimental data. None of the qualitative observations made in section 3.1.1 would change, unless $\alpha > 0$. In this case, the average cargo movement would consist of two diffusive steps, one at the beginning of the motion and one at the end of the first processive step.

3.2.2 myoV–kinesin transport on actin. Using the same assumptions discussed in section 3.1.2, we find the following simplified expression,

$$\langle X_{ap} \rangle = v_a \frac{(\beta(d_a - \mu_a) + (1-\alpha)(k_p + \mu_a)) + d_p(1-\alpha)}{d_a(k_p + \mu_a) + d_p + \mu_a}, \tag{29}$$

indicating a mean run length that decreases linearly as α increases. This is physically expected since we assumed $k_a = 0$, which implies that diffusional states are not allowed to transition to the processive (1,1) state. How $\langle X_{ap} \rangle$ above scales with β depends instead on the difference between μ_a and d_a. The detachment rate of myoV from actin in state (1,0) is about $0.6\ s^{-1}$, and we see from Fig. 5 that this value is never reached (we also verified this result asymptotically). Then, the mean run length of the cargo complex is a decreasing function of the probability of being in state (1,0) at time $t = 0$.

The overall effect of a higher value of β is to lower the best-fit value of d_a and to reduce the range of physically meaningful parameters, as shown in Fig. 7. Similar to what we mentioned in section 3.2.1, the experimental data can be fit to all possible initial conditions. However, if d_p is too small, the condition for the mean run length from ref. 23 cannot be satisfied if β is too large. This is reflected by the negative values of the $\beta = 0.5$ fit to d_a in Fig. 7. These results reinforce the notion that the increased processivity of myoV due to the presence of kinesin depends on the latter's ability to keep the active motor attached to the track for a longer period of time.

3.3 Sensitivity analysis

We conclude this section by performing both local and global sensitivity analysis of our model output on the model parameters. Since our goal is to determine the effect of cooperation among different molecular motors on the processivity of cargo transport, we select $\langle X_{ap} \rangle$ (*e.g.* the mean run length before detachment) as the output of interest.

The simplest local sensitivity analysis evaluates the partial derivatives of the mean run length before detachment with respect to each of the unknown parameters (*e.g.* $\partial \langle X_{ap} \rangle / \partial d_p$).

This determines how sensitive the output is to quantitative changes in each of the kinetic parameters.[27]

Since local sensitivity analysis is best suited to evaluating output that is linear in the parameters, we will also consider global sensitivity analysis on $\langle X_{ap}\rangle$. This analysis will determine which, among the unknown parameters of the model, would be most responsible for experimental variation of the output.[28] This analysis is global in the sense that it spans all of the parameter space. It is model-free, and gives the same result as local sensitivity analysis if the analyzed models are linear.[28] Let us write $\Omega = \{\mu_p,\mu_a,d_p,d_a,k_p,k_a,v_a\}$ as the input space, and Ω_i, $i = 1,2,\ldots,7$ as i-th input in Ω. Then we can define the first-order sensitivity for a fixed input Ω_i as:

$$S_i \equiv \frac{V[E(\langle X_{ap}\rangle|\Omega_i)]}{V[\langle X_{ap}\rangle]}, \qquad (30)$$

where $E(\langle X_{ap}\rangle|\Omega_i)$ is the expected value of the mean run length obtained by uniformly sampling over all other parameters $\Omega_{j\neq i}$, $V[E(\langle X_{ap}\rangle|\Omega_i)]$ is the variance of the expected mean run length over the parameter Ω_i, and $V[\langle X_{ap}\rangle]$ is the unconditional variance of the mean run length. The parameter with highest first order sensitivity index is the one which most influences the variation of the mean run length according to the global sensitivity analysis approach. Global sensitivity analysis can also be used to assess the joint effect of more than one input. We define the second order sensitivity (also known as two-way interaction) as

$$S_{ij} \equiv \frac{V[E(\langle X_{ap}\rangle|\Omega_i,\Omega_j)]}{V[\langle X_{ap}\rangle]}, \qquad (31)$$

where $E(\langle X_{ap}\rangle|\Omega_i,\Omega_j)$ is the expected value of the mean run length given fixed values of Ω_i and Ω_j. Higher order global sensitivity indexes can be analogously defined. We apply local and first and second order global sensitivity analyses to both experimental cases:

3.3.1 myoV–kinesin transport on MT. Representative results of the local sensitivity analysis for the microtubule case are plotted in Fig. 8. Under certain regimes, μ_p has the greatest influence on the mean run length before detachment, followed by d_p, with k_p as the least influential among the three parameters. To further investigate the results from the local sensitivity analysis, we determine the first and second order global sensitivity indexes for all free parameters. These results are listed in the first row of Table 3. We find that the parameter that is responsible for most of the variation in $\langle X_{ap}\rangle$ is d_p.

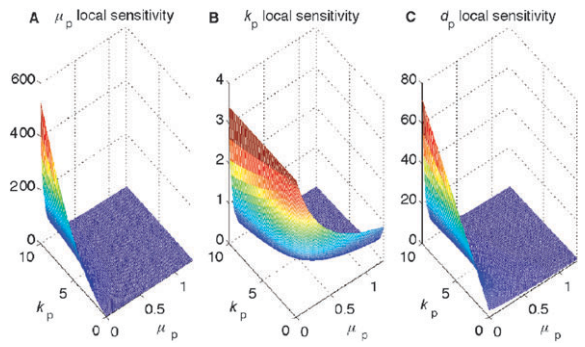

Fig. 8 Local sensitivity analysis of free model parameters in the case of kinesin/myoV cargo transport on microtubules. The parameters for all three of these graphs are $v_a = 0.88\ \mu m\ s^{-1}$, $d_a = \mu_a = 0.52\ s^{-1}$, $k_a = 1.48\ s^{-1}$, and $d_p = 0.5\ s^{-1}$. A: Sensitivity analysis with respect to μ_p, in this case the z-axis represents $\partial\langle X_{ap}\rangle/\partial\mu_p$. B: Sensitivity analysis with respect to k_p, in this case the z-axis represents $\partial\langle X_{ap}\rangle/\partial k_p$. C: Sensitivity analysis with respect to d_p, in this case the z-axis represents $\partial\langle X_{ap}\rangle/\partial d_p$.

Both of the analyses predict that k_p has the least influence on the mean run length, but they differ in their ranking of μ_p and d_p. This difference arises from the nonlinearity of eqn (19) and the intrinsic differences among the two types of analyses. Local sensitivity analysis suggests that if we could control the values of the parameters of the system, we would affect the largest changes in $\langle X_{ap}\rangle$ by altering the rate of detachment of myoV while in state (0,1). If experimentally, we are sampling parameter space, global sensitivity analysis predicts that by correctly determining d_p we can achieve the most reduction in the variability of the mean run length.

Table 3 First and second order sensitivity indexes for microtubule and actin cargo transport. To determine these indexes we sampled d_p and k_p uniformly in [0,20] with step 0.05. For the microtubule case we sampled μ_p in [0,1.25] with step 0.01. For the actin case we sampled d_a in [0,0.42] with step 0.01

Filament type	S_{k_p}	S_{d_p}	S_{μ_p}	S_{d_a}	S_{k_p}	S_{k_p}	S_{d_p}	S_{d_a}	S_{d_a,d_p}
Microtubule	0.06	0.27	0.1	—	0.20	0.35	0.82	—	—
Actin	0.1	0.33	—	0.23	—	0.45	—	0.37	0.81

3.3.2 myoV-kinesin transport on actin. The local and global sensitivity analyses also give different results in the case of cargo transport along actin filaments. Three representative plots of the local sensitivity analysis are shown in Fig. 9. These show that the detachment rate of myoV from actin when both motors are attached is the most influential parameter with respect to the mean run length before detachment. However, the first order sensitivity index of d_a is about 1/3 smaller than the same index for d_p (see Table 3), making the detachment rate of kinesin when in state (1,1) the parameter more

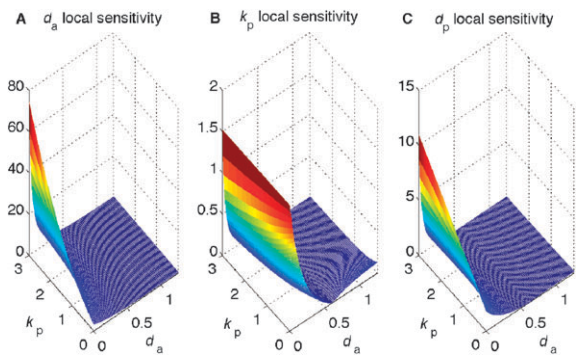

Fig. 9 Local sensitivity analysis of free model parameters in the case of myoV/kinesin cargo transport on actin. The parameters for all three of these graphs are $v_a = 0.46\ \mu m\ s^{-1}$, $\mu_a = 0.6\ s^{-1}$, $k_a = 0\ s^{-1}$, $\mu_p \ll 1$ and $d_p = 0.5\ s^{-1}$. A: Sensitivity analysis with respect to μ_p, in this case the z-axis represents $\partial\langle X_{ap}\rangle/\partial d_a$. B: Sensitivity analysis with respect to k_p, in this case the z-axis represents $\partial\langle X_{ap}\rangle/\partial k_p$. C: Sensitivity analysis with respect to d_p, in this case the z-axis represents $\partial\langle X_{ap}\rangle/\partial d_p$.

responsible for the variance in $\langle X_{ap} \rangle$. In this case, the sensitivity to d_p is consistent with the role of the passive tether in preventing myoV detachment.

Interestingly, both cases (actin and microtubule) have d_p as the free parameter with highest first order sensitivity and k_p as the lowest one. Moreover, if we want to reduce by at least 80% the uncertainty in the determination of the mean run length, we can do so by exactly determining d_p and μ_p for the microtubule case and d_p and d_a for the actin case (*cf*. Table 3).

4. Summary & conclusions

We presented a stochastic model that describes the cooperative behavior between two different motors attaching cargoes to a cytoskeletal filament. Of the two motors, one acts as an engine, moving the cargo unidirectionally along the filament, while the other acts as a tether. Although we computed the full cargo run length and cargo run time probability distribution functions associated with our model, since only mean run lengths and run times were quantitatively measured,[23] we fit our model only using these means.

Experimental visualization indicates significant diffusive dynamics for cargo transport along microtubules in the presence of myosin V, while cargoes transported along actin did not exhibit diffusive dynamics. A consistent interpretation of these observations is that along microtubules, tethers (myosin) predominantly enhance reattachment of the active motor (kinesin). In the case of transport along actin, the kinesin tether acts to prevent detachment of the active myosin motor. This interpretation has been verified within our model when fit only to the measured mean run lengths and run times. In fact, for the case of microtubule transport we found that the reattachment rate (k_a) of kinesin to the filament when the tether is attached is three times faster than its corresponding detachment rate. For the case of actin, we found that the detachment rate of myoV when kinesin is attached to the filament is slower than in the absence of the tether for all values in the explored parameter space. Even though we fit only to the means, as shown in Fig. 2, using parameters among those consistent with the fitting (Fig. 4–7), the PDFs for transport along microtubules and along actin differ qualitatively. The PDF for transport along microtubules are much broader than those for transport along actin, indicating more frequent diffusive motion of microtubule transport, and qualitatively consistent with experimental observations. Qualitatively differing PDFs have also been proposed for a different biophysical system.[29] We expect that our parameter space can be further constrained by fitting the variances (second moments) of the run length and run time PDFs provided systematic, quantitative measurements are taken. The physicochemical reasonableness of such further constrained parameter sets would provide an additional test of our model.

Acknowledgements

The authors are grateful to Y. Ali, H. Lu, and D. Warshaw for their clarifying comments. This work was supported by grants from the NSF (DMS-0349195, DMS-0719462) and the NIH (K25 AI41935).

References

1 R. D. Vale, *Cell*, 2003, **112**, 467.
2 R. Mallik and S. P. Gross, *Physica A*, 2006, **372**, 65.
3 H. Lodish, A. Berk, P. Matsudaira, C. A. Kaiser, M. Krieger, M. P. Scott, S. L. Zipursky and J. Darnell, W.H. Freeman Co, 5th edn, 2005.
4 S. P. Gross, *Curr. Biol*., 2007, **17**, R277.
5 M. A. Welte, *Curr. Biol*., 2004, **14**, R525.
6 A. D. Metha, R. S. Rock, M. Rief, J. A. Spudich, M. S. Mooseker and R. E. Cheney, *Nature*, 1999, **400**, 590.
7 S. P. Gross, M. Vershinin and G. T. Shubeita, *Curr. Biol*., 2007, **17**, R478.
8 S. M. Block, L. S. B. Goldstein and B. J. Schnapp, *Nature*, 1990, **348**, 348.
9 K. Visscher, M. J. Schnitzer and S. M. Block, *Nature*, 1999, **400**, 184.
10 K. Shiroguchi and K. Kinosita Jr., *Science*, 2007, **316**, 1208.
11 M. Rief, R. S. Rock, A. D. Mehta, M. S. Mooseker, R. E. Cheney and J. A. Spudich, *Proc. Natl. Acad. Sci. U. S. A*., 2000, **97**, 9482.
12 N. J. Carter and R. A. Cross, *Nature*, 2005, **435**, 308.
13 K. Svoboda and S. M. Block, *Cell*, 1994, **77**, 773.
14 K. Kawaguchi and S. Ishiwata, *Biochem. Biophys. Res. Commun*., 2000, **272**, 895.
15 A. E. Clemen, M. Vilfan, J. Jaud, J. Zhang, M. Barmann and M. Rief, *Biophys. J*., 2005, **88**, 4402.
16 M. E. Fisher and A. B. Kolomeisky, *Physica A*, 1999, **274**, 241.
17 A. B. Kolomeisky and M. E. Fisher, *Biophys. J*., 2003, **84**, 1642.
18 K. I. Skau, R. B. Hoyle and M. S. Turner, *Biophys. J*., 2006, **91**, 2475.
19 A. B. Kolomeisky and M. E. Fisher, *Annu. Rev. Phys. Chem*., 2007, **58**, 675.
20 A. Vilfan, *Biophys. J*., 2008, **94**, 3405.
21 A. Kunwar, M. Vershinin, J. Xu and S. P. Gross, *Curr. Biol*., 2008, **18**, 1173.
22 M. Y. Ali, E. B. Krementsova, G. G. Kennedy, R. Mahaffy, T. D. Pollard, K. M. Trybus and D. M. Warshaw, *Proc. Natl. Acad. Sci. U. S. A*., 2007, **104**, 4332.
23 M. Y. Ali, H. Lu, C. S. Bookwalter, D. M. Warshaw and K. M. Trybus, *Proc. Natl. Acad. Sci. U. S. A*., 2008, **105**, 4691.
24 A. P. Alivisatos, W. Gu and C. Larabell, *Annu. Rev. Biomed. Eng*., 2005, **7**, 55.
25 L. S. Milescu, A. Yildiz, P. R. Selvin and F. Sachs, *Biophys. J*., 2006, **91**, 3135.
26 S. Klumpp and R. Lipowsky, *Proc. Natl. Acad. Sci. U. S. A*., 2005, **102**, 17284.
27 A. Saltelli, M. Ratto, S. Tarantola and F. Campolongo, *Chem. Rev*., 2005, **105**, 2811.
28 A. Saltelli, S. Tarantola, F. Campolongo and M. Ratto, W.H. Freeman Co, 5th edn, 2005.
29 M. Voliotis, N. Cohen, C. Molina-París and T. Liverpool, *Biophys. J*., 2008, **94**, 334–348.

